

Nanoscale

Accepted Manuscript



This is an *Accepted Manuscript*, which has been through the Royal Society of Chemistry peer review process and has been accepted for publication.

Accepted Manuscripts are published online shortly after acceptance, before technical editing, formatting and proof reading. Using this free service, authors can make their results available to the community, in citable form, before we publish the edited article. We will replace this *Accepted Manuscript* with the edited and formatted *Advance Article* as soon as it is available.

You can find more information about *Accepted Manuscripts* in the [Information for Authors](#).

Please note that technical editing may introduce minor changes to the text and/or graphics, which may alter content. The journal's standard [Terms & Conditions](#) and the [Ethical guidelines](#) still apply. In no event shall the Royal Society of Chemistry be held responsible for any errors or omissions in this *Accepted Manuscript* or any consequences arising from the use of any information it contains.



Nanoscale

ARTICLE

Polymeric Capsule-Cushioned Leukocyte Cell Membrane Vesicles as a Biomimetic Delivery Platform

Changyong Gao, Zhiguang Wu, Zhihua Lin, Xiankun Lin, and Qiang He*

Received 00th January 20xx,
Accepted 00th January 20xx

DOI: 10.1039/x0xx00000x

www.rsc.org/

We report a biomimetic delivery of microsized capsule-cushioned leukocyte membrane vesicles (CLMVs) through the conversion of freshly reassembled leukocytemembrane vesicles (LMVs), including membrane lipids and membrane-bounded proteins onto the surface of layer-by-layer assembled polymeric multilayer microcapsules. The leukocyte membrane coating were verified by using electron microscopy, quartz crystal microbalance, dynamic light scattering, and confocal laser scanning microscopy. The resulting CLMVs have the ability to effectively evade clearance by the immune system and thus prolong the circulation time in the mice. Moreover, we also show that the right-side-out leukocyte membrane coating can distinctly improve the accumulation of capsules in tumor site through the molecular recognition of membrane-bounded proteins of CLMVs with those of tumor cells *in vitro* and *in vivo*. The nature cell membrane camouflaged polymeric multilayer capsules with the immunosuppressive and tumor-recognition functionalities of natural leukocytes provides a new biomimetic delivery platform for disease therapy.

Introduction

The development of an intelligent biomimetic micro-/nanocapsule system that can be utilized for molecular sensing or delivery applications in biology and medicine is of great interest.^[1-5] Particularly, layer-by-layer (LbL) assembled polyelectrolyte capsule-based “artificial cell” systems have been recently considered for such applications owing to the outstanding capacity to facilitate localized release of encapsulated molecules on demand.^[6-12] These LbL-assembled polyelectrolyte capsules that mimic compartmentalization of natural cells have well-controlled size, shape and wall thickness.^[13, 14] The wall composition can be readily changed to adjust their physicochemical property,^[15-19] and the encapsulated components inside capsules can be released as a consequence of externally or internally physiochemical and biological stimuli.^[20-23] Through the conversion of liposomes into lipid bilayers to cover the capsules’ surface,

polyelectrolyte capsule-supported liposomes that greatly improve the stability and lifetime of lipid membranes have also been considered as an ideally supported biomimetic membrane system to study the biophysical properties of real cell membranes and membrane-bounded proteins.^[24, 25] More importantly, the fused lipid membranes in analogue to the cell membrane could enhance the ability that tunes the permeability of LbL-assembled capsules,^[26, 27] and also provide a cushion to host specific units for targeted tumor recognition.^[28] To date, great effort has been focused on *in vitro* experiments of drug encapsulation and release, but *in vivo* experiments of microcapsules for cancer therapy are still relatively rare. We have recently demonstrated that folate-lipid bilayer modified hollow polyelectrolyte microcapsules can be systematically circulated in the mouse through the intravenous injection due to their good deformability similar to microsized red blood cells.^[29] However, there are still a large proportion of microcapsules that is adsorbed by liver and other immune organs. Therefore, current polyelectrolyte capsule-supported liposomes require the separation or synthesis of specific recognition units, and also have not yet reached its full therapeutic potential in practice owing to unavoidable opsonization and non-specific clearance *in vivo*.^[30, 31]

State Key Laboratory of Robotics and System (HIT), Micro/Nanotechnology Research Center, Harbin Institute of Technology, Yikuangjie 2, Harbin 150080, China

E-mail: qianghe@hit.edu.cn

*Electronic Supplementary Information (ESI) available. See DOI: 10.1039/x0xx00000x

ARTICLE

Nanoscale

Human blood cells including erythrocytes (i.e., red blood cell) and leukocytes (i.e., white blood cell) are nature's long-circulating delivery vehicles, which has inspired the engineering of blood cells-based artificial delivery systems.^[32-36] For example, erythrocyte membranes have been derived to reassemble and encapsulate synthetic nanoparticles which exhibited superior circulation half-life compared to their PEGylated counterparts.^[37] In contrast with erythrocyte membranes without any specific targeting ligands, leukocytes not only process long blood-circulating time but also can cross the biological barriers of the body, recruit and localize at the targeted tissues because leukocytes have a variety of proteins residing on the membranes for discerning inflammation and diseased region.^[38-41] With the aim of engineering polyelectrolyte capsules with improved functions and advanced biomimetic features, we herein report an elegant strategy in polyelectrolyte capsules' biofunctionalization by using the entire functional utility of a natural leukocyte cell membrane. After bioactive leukocyte cell membrane vesicles reconstructed from freshly harvested leukocytes were transformed onto the surface of biocompatible hollow polyelectrolyte multilayer capsules, polyelectrolyte capsule-cushioned leukocyte cell membrane vesicles or leukocyte cell membrane-camouflaged polyelectrolyte capsules were obtained. Such a biocompatible system more closely mimics the surface properties of parent leukocytes and provides a platform for the creation of smart biomimetic delivery vessels for avoiding clearance by the mononuclear phagocyte system, overcoming the vascular barrier, and localizing at the target tissue in sufficient quantities to be effective.

Experimental

Materials and Cell Culture

Silica spheres with diameters of 2.5 μm were purchased from Microparticles GmbH, Berlin, Germany. Chitosan (CHI, Medium molecular weight), sodium alginate (ALG, Low viscosity), fluorescein isothiocyanate (FITC), 2-(4-Amidinophenyl)-6-indolecarbamidine dihydrochloride 4',6-Diamidino-2-phenylindole dihydrochloride (DAPI), Doxorubicin hydrochloride (DOX), 3-(4,5-Dimethylthiazol-2-yl)-2,5-diphenyl

tetrazolium bromide (MTT) were obtained from Sigma Aldrich. 1,1'-dioctadecyl-3,3,3',3'-tetramethylindodicarbocyanine perchlorate (DiD), Roswell Park Memorial Institute (RPMI) 1640 medium (RPMI 1640), Dulbecco's Modified Eagle's Medium (DMEM), 0.25% Trypsin-EDTA, penicillin streptomycin and no mycoplasma fetal bovine serum (FBS) were purchased from Life Technologies Corporation. All chemicals were analytic grade and were used without further purification. Murine J774A phagocytic cells and human cervical cancer HeLa cell lines were purchased from the American Type Culture Collection (ATCC). All cells were cultured according to the vendor directions.

Preparation of LbL-assembled capsules

Well-dispersed (ALG/CHI)₈ capsules were prepared by the layer-by-layer assembly of polyelectrolyte layers on the surface of SiO₂ particles with a diameter of 2.5 μm . Firstly, the particles were suspended in 2 mg mL⁻¹ CHI solution containing 0.5 M NaCl for 15 min under continuous shaking, excess polyelectrolytes were removed by centrifugation and washed three times using 0.1 M NaCl. The CHI-coated silica particles were suspended in 2 mg mL⁻¹ ALG solution containing 0.5 M NaCl for 15 min under continuous shaking and then repeated the above CHI/ALG deposition procedure. Then 1 M HF was used to remove the silica template. Hollow capsules were purified by five centrifugation/water washing steps. All prepared capsules solutions were stored at 4°C. For *in vivo* fluorescence imaging, Cy7, a near-infrared fluorescent probe, was labelled to CHI, and the Cy7-capsules were prepared using the procedures described above. Hollow capsules were characterized by scanning electron microscopy (SEM, Hitachi S4800), transmission electron microscopy (TEM, FEI Tecnai G2 20S-TWIN) and laser scanning confocal microscopy (CLSM, Leica TCS SP5).

Isolation of the leukocyte membrane

The isolation of the cellular membrane was performed according to a previous report.^[32] To harvest membrane, cells were harvested and washed with PBS. Then the cells were suspended in a hypotonic lysing buffer consisting of 1 mM NaHCO₃, 0.2 mM EDTA and 1 mM PMSF in 4°C cover night,

repeated grinding cell suspended solution using a Dounce homogenizer with a tight-fitting 20 times before 3200 g for 5 min at 4°C centrifuge and remove pellet. The resulting supernatant were centrifuged at 15000 g for 30 min at 4°C, the pellet was plasma membrane. As-prepared isolated membranes were dispersed in PBS (pH 7.4).

CLMVs synthesis

To synthesis CLMVs, previously reported method was used.^[37] The isolated leukocyte cell membranes were sonicated at 4°C for 10 min under the condition of 59 kHz and 100 W using a bath sonicator. The resulted membranes were physically extruded through 100 nm polycarbonate for 15 passes. Then, 1 mg of capsules were mixed with membrane vesicles prepared from 10⁷ leukocyte cells at least 1 h at 4-10°C under a sonicate frequency of 59 kHz. The CLMVs were separated by centrifugation at 5000 rpm for 2 min and residual membranes were discharged.

Characterization of CLMVs

TEM imaging was carried out by dropping 0.5 mg mL⁻¹ CLMVs on the grid of carbon-coated 400 nm square mesh copper grids. After 10 min, grids were negatively stained with 3 drops of 1% uranyl acetate. The samples were imaging at 200 kV. A Zetasizer (Malvern) was used to take dynamic light scattering (DLS) measurement for the characterization of zeta potential. Samples were suspended in water at 0.5 mg mL⁻¹. Serum stability tests were conducted by suspending the capsules and CLMVs in 100% FBS with a final concentration of 0.5 mg mL⁻¹. Samples were incubated at 37°C. The absorbance at 560 nm was measured periodically.

Cytotoxicity of CLMVs

Normal hepatic (L02) cells were used for cytotoxicity studies. When cells in 96-well plates were cultured at a concentration about 90%, 0.1 mg CLMVs or bare capsules were added. Cell survival was studied by the standard MTT assay. Specifically, after incubation for 24 h, the cultured medium was removed and replaced. MTT (10 µL, 0.5 mg mL⁻¹) in PBS was added and incubated at 37°C for 4 h. Then the remaining MTT was changed to DMSO (150 µL) to solubilize the purple formazan

crystals. After 10 min, the wells were characterized at a wavelength of 490 nm by using aiMark Microplate Reader (Bio-Rad).

QCM-measurements

Quartz sensors were coated with same polyelectrolyte layers of capsules adsorbed from polyelectrolyte solutions circulating at a flow rate of 75 µL min⁻¹ and at 25°C. After equilibration from water to PBS, J774 cell membrane vesicles in PBS (0.1 mg mL⁻¹) were delivered into the measuring chamber. The formation of the leukocyte membrane vesicles was monitored in real time (qCell T, 3T analytik, Germany).

Flow cytometry analysis

J774 cells were cultured at a concentration about 75% in 25 cm² flasks and co-incubated with capsules and CLMVs (tagged with FITC respectively) at cell: capsules ratios of 1:4. After 2 h, samples were washed 3 times with PBS to remove non-adherent capsules. Cells were harvested by scraping and treated with Trypan Blue (0.04%) to quench their surface fluorescence. Flow cytometry was performed using a BD FACS Aria.

Circulation half-life study

Male BALB/c nude mice, aging 4 weeks were purchased from Vital River Laboratories (VRL, Beijing, China). All the animal procedures were carried out under the guidelines and approved by the local ethics committee. To evaluate the circulation half-life of CLMVs, 100 µL of 2 mg mL⁻¹ FITC-capsules or FITC-CLMVs were injected into mice through tail-vein injection. Following the injection, 25 µL of blood were collected from the eye socket of the mice at 1, 2, 4, 6, 8, 12, 16, 20 and 24 h for fluorescence intensity tests.

Cell binding ability

J774 cells were labelled using DiD for 15 min, followed by washing with PBS for five times to clean the residual DiD. Then, DiD labelled J774 cells were co-cultured with HeLa and L02 cells. After 6 h, the unbinding J774 cells were washed away with PBS for 3 times. The cells were visualized using CLSM.

Cancer cell binding study

Hela cells were plated at 75% concentration in Confocal Petri Dish. Cells were washed using PBS and incubated with 1640 medium before adding 0.5 mg of FITC and DiD labelled CLMVs or bare FITC labelled capsules. The capsules were incubated with cells for 3 h at 37°C. The cells were washed with PBS 5 times, and then stained with DAPI. The cells were visualized by using CLSM. Digital images of green, red, and blue fluorescence were acquired under FITC, Cy5 and DAPI filters respectively.

In vivo experiment

Male BALB/c nude mice aging 4 weeks were purchased from Vital River Laboratory Animal Center (Beijing, China). All of the animal experiments were performed under the protocols approved by the Institutional Animal Care and Use Committee of HIT (Harbin Institute of Technology). Tumor bearing mice model was established by inoculating 10^7 human cervical Hela cells in the site of leg of each mouse. When the volume of tumor reached about 100 mm^3 , 200 μL of Cy7-capsules or Cy7-CLMVs solution (4 mg mL^{-1}) was injected into mice via the tail vein. After injection for 1 h, 4 h, 8 h, 12 h and 24 h, near-infrared mice images were captured using a Kodak *in vivo* imaging system (Care stream Health Inc). After 24 h, all the mice were euthanized. Tumors and organs were removed and washed with PBS followed by ex vivo fluorescence imaging.

Preparation of Frozen Section

Tumor bearing mice were injected with 200 μL of FITC-Capsules or FITC-CLMVs at a concentration of 4 mg mL^{-1} . Mice were euthanized after 24 h and the tumors were collected. The isolated tumors were cut into 7 μm slices. Sections were stained using DAPI and observed using a Leica TCS SP5 II confocal microscopy.

Results and Discussion

As illustrated in Fig. 1A, the preparation process of camouflaging capsules with leukocyte cell membranes is composed of three steps: preparing hollow polyelectrolyte multilayer capsules through template-assisted LbL assembly,

reassembling membrane vesicles from freshly harvested leukocytes and fusing the vesicles onto the surface of polyelectrolyte multilayer capsules. Here, hollow polyelectrolyte multilayer capsules were prepared following previously published procedures, consisting of eight bilayers of alternating sodium alginate (ALG) and chitosan (CHI) via the template-assisted LbL assembly. Scanning electron microscopy (SEM), transmission electron microscopy (TEM) and confocal laser scanning microscopy (CLSM) of the resulting (ALG/CHI)₈ capsules show well-defined hollow capsule structure and a diameter of around 2.5 μm (Fig. S1). Leukocyte ghosts were prepared from freshly harvested murine J774 cells according to the literatures and extruded through 100 nm porous polycarbonate membranes to produce leukocyte membrane-derived vesicles. To camouflage (ALG/CHI)₈ capsules with leukocyte membranes, (ALG/CHI)₈ capsules (1mg) were mixed with leukocyte membrane vesicles (LMVs) prepared from 10^7 leukocyte cells for at least 1 h by sonication and oscillation.

To test the assembly of LMVs on the (ALG/CHI)₈ surface, quartz crystal microbalance (QCM) was firstly employed (Fig. 1B). The real-time frequency change shows an immediate decrease of 138.36Hz at 5th overtone upon injection of membrane vesicles, indicating rapid adsorbing on the (ALG/CHI)₈ surface. However, the computed thickness of the adsorbed membranes is about 20 nm, which is approximatelytwicetimes than that of single layer of leukocyte membranes (~ 8 nm), suggesting that the adsorbed membranes didnot completely form a single layer without any external actions. Note that the fusion of LMVs on the surface of (ALG/CHI)₈capsules in the following experiments was performed with the aid of strong shaking action so that extra membranes could be removed. Moreover, the changes of surface morphology and surface charge of (ALG/CHI)₈ capsules before and after the membrane camouflaging were monitored. One can see that the surface zeta potential of (ALG/CHI)₈ capsules switched from +36.13 mV to a negative value -31.38 mV upon fusing with J774 cell membrane vesicles, which is almost equal to that of J774 cells (-33.64 mV) (Fig. 1C). A TEM image of the resulting (ALG/CHI)₈ capsules-cushioned LMVs (CLMVs) negatively stained with uranyl acetate in Fig. 1D shows a collapsed capsule structure decorated with lots of approximately 50 nm membrane patches compared to that of

a bare (ALG/CHI)₈ capsule (inset TEM image). Also, the TEM image confirms the formation of a single layer of leukocyte membranes on the surface of (ALG/CHI)₈ capsules, suggesting that the strong shaking is effective enough to wipe off excess membrane patches. To further confirm the cell membrane covering, fluorescein isothiocyanate (FITC, excitation/emission = 488nm/520nm)-labeled CHI (FITC-CHI) was assembled onto the outer layer of capsules, and hydrophobic 1,1'-dioctadecyl-3,3,3'-tetramethylindodicarbocyanine, 4-chloro-benzenesulfonate salt (DiD, excitation/emission = 644nm/655nm) fluorophore was used to label cell membranes. Confocal laser scanning microscopy (CLSM) images show continuous green or red fluorescence circles with diameters of approximately 2.5 μm (Fig. 1E). The green fluorescence comes from FITC-CHI in the shell of (ALG/CHI)₈ capsules and the red fluorescence represents the successful assembly of cell membranes onto the surface of capsules. Overall, these results suggest a successful translocation of natural cell membranes onto the (ALG/CHI)₈ capsules.

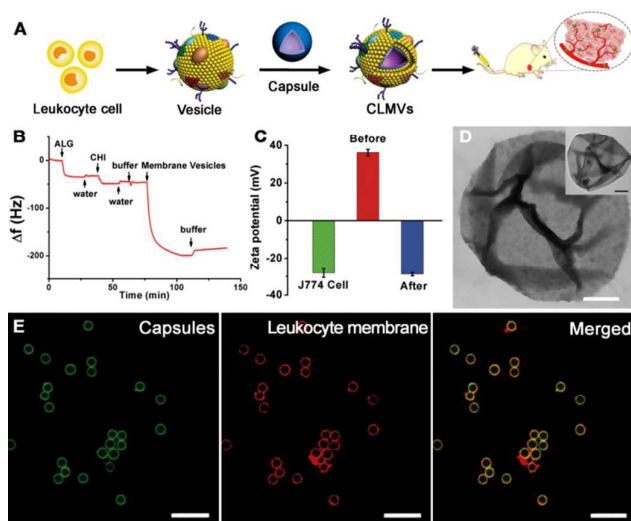


Fig. 1 (A) Preparation process of polymeric capsule-cushioned leukocyte cell membrane vesicles and its potential application in cancer therapy. (B) QCM measurements demonstrating the adsorbing cell membranes vesicles on the LbL-assembled capsules at 5th overtone. (C) Surface zeta potential of the J774 cells, bare capsules and the CLMVs. (D) TEM images of the CLMVs and capsule (inset). Scale bar = 500 nm. (E) CLSM images of the CLMVs demonstrated the colocalization of the capsules (visualized with green FITC dyes) and leukocyte cell membranes (visualized with red DiD dyes). Scale bar = 10 μm .

Next, we investigated their cytotoxicity and their anti-phagocytosis ability against macrophage. In the cytotoxicity experiment, bare (ALG/CHI)₈ capsules and CLMVs were individually incubated with normal hepatocyte (L02) cell lines for 24 h at a concentration of 100 $\mu\text{g mL}^{-1}$. Fig. 2A shows CLMVs did not have an evident impact on the cell viability, and actually the membrane coating slightly increased the biocompatibility of capsules. In the anti-phagocytosis study, FITC-labelled CLMVs and bare FITC-labelled capsules were incubated with equivalent numbers of J774 macrophage cells. After 2 h of incubation, flow cytometry was employed to quantify the capsule internalization (Fig. 2B). The membrane coating was found to significantly decrease the uptake by macrophage compared to bare capsules. These results demonstrate that the membrane coating exhibits low cytotoxicity and greatly decreases the phagocytosis effect by the same source of macrophage cells.

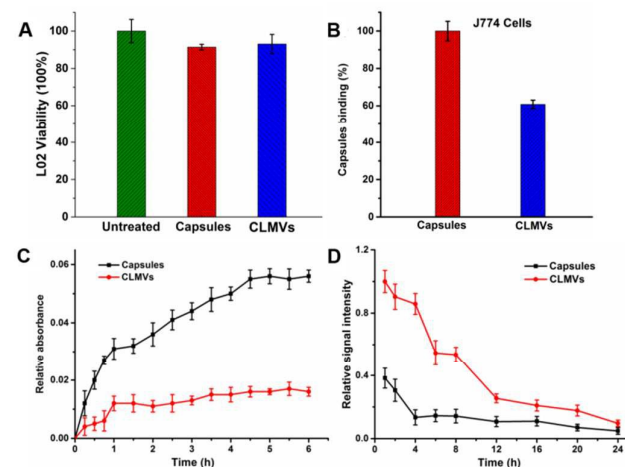


Fig. 2 In vitro cytotoxicity, inhibition of phagocytosis, stability in serum, and the *in vivo* circulation time of the CLMVs. (A) L02 viability post incubation with bare capsules and CLMVs. Measurements were normalized to the viability of untreated cells. (B) Internalization of bare capsules and the CLMVs by J774 cells. (C) Bare capsules and CLMVs were incubated in 100% fetal bovine serum and monitored for absorbance. (D) FITC-labeled capsules and CLMVs were injected intravenously through the tail-vein of mice. At various time points blood was withdrawn and measured for fluorescence to evaluate the systemic circulation lifetime.

Due to the readily serum protein binding of positively charged carriers, which results in size increase and aggregation, carriers usually were cleared from systemic circulation.^[37] To evaluate the serum stability of CLMVs, CLMVs were then examined and uncoated (ALG/CHI)₈ capsules were used as control. The serum stability was carried out following previous reported methods.^[37] Briefly, aggregation of particles induce the increase of light scattering and thus the change of specific absorbance value can be used to monitor the size change of capsules in the presence of fetal bovine serum (FBS). Two types of capsules at a final concentration of 2 mg mL⁻¹ was suspended in 100% FBS at 37 °C. Prior to the absorbance measurement test, samples were shaken gently. The absorbance results indicate that CLMVs have a relative stability in 6 h (Fig. 2C).

We then investigated the *in vivo* systemic circulation time of CLMVs and uncoated (ALG/CHI)₈ capsules by using flow cytometry. The FITC was used as a marker for the flow cytometry experiment since FITC-labelled CHI could be easily assembled onto the wall of capsules. For each type of capsules, 100 µL of 2 mg mL⁻¹ FITC-labelled capsules were injected into a group of mice through tail-vein injection. At various time points after injection, 25 µL of blood was collected from the eye socket of the mice for fluorescent test. The fluorescence measurement at 488 nm (Fig. 2D) shows that CLMVs have stayed a longer time during blood circulation than uncoated (ALG/CHI)₈ capsules. More interestingly, the uncoated (ALG/CHI)₈ capsules have almost been eliminated after 4 h of treatment. In contrast, (ALG/CHI)₈ capsule-cushioned LMVs displayed 85%, 52% and 25% retention after 4 h, 8 h and 12 h, respectively. The relatively short circulation time *in vivo* of the uncoated capsules was attributed to rapid aggregations in serum and clearance by the immune system. Furthermore, the half-life of CLMVs was estimated to be 8.4 h, which further confirms that the functional components of cell membrane vesicles can prevent immune clearance. This evidence further confirms that the opsonization of capsules and subsequent specific clearance are effectively inhibited by the J774 membrane coating. Therefore, the CLMVs appear to have longer *in vivo* circulating time compared to the bare (ALG/CHI)₈ capsules. It is worthy to be mentioned that the intravenously

injected microparticles are immediately cleared from the blood circulation and predominantly distributed into the capillary beds in the lungs and other organs.^[42] Interestingly, blood cells including erythrocytes and leukocytes can easily pass through capillaries with dimensions smaller than their size and have a long circulation time in living organisms, which is largely described to their deformable behaviour and ability.^[43, 44] Recently soft hydrogel microparticles or polymer microcapsules with moderate modulus have been demonstrated to have longer circulation time in living organisms behaving like RBCs.^[45]

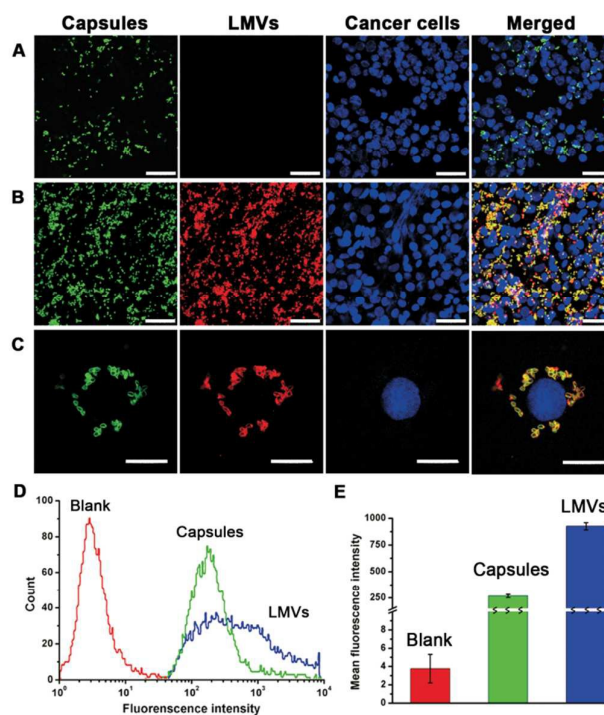


Fig. 3 CLSM images demonstrated the tumor binding of (A) bare capsules, (B) and (C) CLMVs. After incubated with HeLa cells for 3 h, the excess capsules were washed out, and the cells were subsequently fixed for imaging. Scale bar = 50 µm (A, B), 20 µm (C). (D) Flow cytometry analysis of HeLa cells. (E) Quantification of the mean fluorescence intensities of the binding in (D).

Many studies have demonstrated that monocytes and phagocytes tend to accumulate onto tumors owing to the collective contribution of multiple membrane components on the cell surfaces.^[39] Here, L02 and HeLa cells were individually cultured with DiD-labeled J774 cells for 6 h. It was found that HeLa cells gathered more J774 cells than L02 cells, confirming

the ability of J774 cells bind to tumor cells (Fig. S2). In this case, the resulting CLMVs are expected to inherit such surface recognition functionality. To test it, these engineered capsules were incubated with HeLa cells. After 3 h of incubation, the excess capsules were washed out, and the cells were subsequently fixed for CLSM imaging. Note that a blue-fluorescent probe 4',6-diamidino-2-phenylindole (DAPI) was used to label HeLa cells and similarly a green-fluorescent FITC-CHI was assembled onto the shell of capsules. Fig. 3A shows that only a small number of uncoated capsules were bound onto HeLa cells. In contrast, Fig. 3B shows that nearly all of HeLa cells accumulated different amount of the CLMVs, which was further confirmed by the enlarged CLSM images in Fig. 3C.

We then continued to employ flow cytometry to quantitatively evaluate the binding difference between two capsules. One can see that HeLa cells treated with CLMVs showed a prominent right shift upon cytometric analysis, suggesting greater cellular binding of the CLMVs (Fig. 3D). Fig. 3E demonstrates that nearly 100% of HeLa cells had increased fluorescence except the control group, and the binding ability of CLMVs is four times to uncoated capsules, indicating that the J774 membrane coating greatly improves the target efficacy. In general, these results show the successful translocation of tumor-accumulation functionality from murine J774 cells onto the CLMVs.

Finally, we assessed the feasibility of the CLMVs for *in vivo* accumulating to the tumor in a mouse model bearing HeLa tumor on the leg. To monitor the distribution of both Cy7-capsules and Cy7-CLMVs, a near-infrared fluorescent dye, Cyanine 7 (i.e. Cy7) with an excited wavelength of 750 nm was used. When the volume of tumor reached about 100 mm³, 200 μ l of Cy7-capsules or Cy7-CLMVs solution was injected intravenously via the tail vein and then *in vivo* fluorescence imaging was conducted at different time points, including 1 h, 4 h, 8 h, 12 h and 24 h injection (Fig. 4A). It was found that after 1 h of injection, Cy7 fluorescence was observed in the whole body and the fluorescence intensity in the tumor sites (both capsule and CLMVs treated one) was significantly increased for 4 h postinjection, indicating that both bare capsules and CLMVs could be accumulated in the tumor site. As time elapsed, however, the fluorescence intensity of tumors in the CLMVs treated one was notably higher than that

of the bare capsule group, suggesting that the existing surface proteins on the CLMVs enhanced the active targeting ability by recognizing tumor endothelium and thus greatly improved tumortropic accumulation. These *in vivo* experimental results is fairly in agreement with the previous cell experiments in Fig. 3.

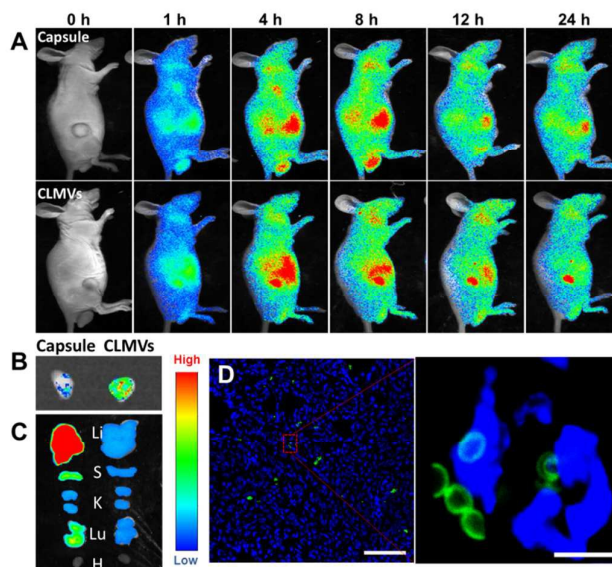


Fig. 4 Evaluation of the CLMVs accumulating to the tumor *in vivo*. (A) *In vivo* fluorescence images of the mice with armpit tumors derived from HeLa cells after the tail vein injection of Cy7-CLMVs or Cy7-Capsules for 1, 4, 8, 12 and 24 h, respectively. (B, C) *Ex vivo* fluorescence images of the tumors and other organs (Li, liver; S, spleen; K, kidney; Lu, lung; H, heart) for 24 h injection. (D) Frozen sections of the tumors after 24 h of the FITC-CLMVs injection. Particles are shown in green (FITC channel), and cell nuclei stained blue (DAPI channel). Scale bar = 50 μ m (D), 5 μ m (the enlarged one).

More importantly, strong fluorescence signal was still observed in the tumor of CLMVs treated mice for 24 h postinjection. The fluorescence of excised tumors *ex vivo* further confirms that the CLMVs accumulated higher amount than the bare capsules to the tumor sites (Fig. 4B). Compared to the bare capsules treated group, less CLMVs in the CLMVs treated group were taken up by liver, spleen, kidney, lung, and heart (Fig. 4C), indicating that the leukocytes membrane coating effectively decrease the accumulation in the reticuloendothelial system (RES), which is entirely consistent

ARTICLE

Nanoscale

with the above-mentioned longer circulation results in **Fig. 2D**. Further tissue section studies have been performed to determine the distribution of CLMVs in the tumor.^[46] The CLSM images of the tumor frozen section for 24h postinjection in **Fig. 4D** shows that the CLMVs have entered into the tumor tissue. Here, the green colour comes from the FITC-labelled CLMVs and the blue colour represents the DAPI stained tumor cell nuclei. Interestingly, the enlarged CLSM image shows a deformable and ellipsoidal capsule structure, confirming that the resulting microsized CLMVs have good deformation ability like that of blood cells owing to higher osmotic pressure during blood circulation.

Conclusions

We have demonstrated a bioinspired camouflage (“top-down”) strategy to functionalize LbL-assembled (“bottom-up”) polymeric multilayer microcapsules with cellular membranes derived directly from freshly natural leukocyte cells, yielding stable, microsized capsule-cushioned leukocyte membrane vesicles. The resulting microsized capsule-cushioned leukocyte membrane vesicles greatly improve the stability and lifetime of membrane vesicles, and inherit the immunosuppressive functionalities of mother cells for decreasing the opsonization and non-specific clearance. Also, these microsized particles exhibit long blood retention and circulation time, which are caused by the leukocyte membrane camouflage, and their good deformability behavior and ability like those microsized blood cells. It is interesting to note that the right-side-out leukocyte membrane coating markedly enhances the targeted accumulation of capsules around tumor cells and the ability to tune the permeability of LbL-assembled capsules. Our flexible approach of using biologically inspired components to build integrated systems could provide important new directions for treating diseases *in vivo*. Furthermore, the resulting microsized capsule-cushioned leukocyte membrane vesicles can be also considered as an ideally supported biomimetic membrane system to regenerate some cellular processes in a man-made environment, and further study the biophysical properties of real cell membranes and membrane-bounded proteins.

Acknowledgements

This work was financially supported by the National Science Foundation of China (21573053) and State Key Laboratory of Robotics and System (HIT).

Notes and references

- 1 J. W. Yoo, D. J. Irvine, D. E. Discher, S. Mitragotri, *Nat. Rev. Drug Discovery*, 2011, **10**, 521.
- 2 X. Huang, M. Li, D. C. Green, D. S. Williams, A. J. Patil, S. Mann, *Nat. Commun.*, 2013, **4**, 3239.
- 3 M. Marguet, C. Bonduelle, S. Lecommandoux, *Chem. Soc. Rev.*, 2013, **42**, 512.
- 4 Q. He, Y. Cui, J. B. Li, *Chem. Soc. Rev.* 2009, **38**, 2292.
- 5 C. M. J. Hu, R. H. Fang, J. Copp, B. T. Luk, L. F. Zhang, *Nat. Nanotechnol.*, 2013, **8**, 336.
- 6 E. Donath, G. B. Sukhorukov, F. Caruso, S. A. Davis, H. Mohwald, *Angew. Chem., Int. Ed.*, 1998, **37**, 2202.
- 7 T. M. S. Chang, *Nat. Rev. Drug Discovery*, 2005, **4**, 221.
- 8 B. Stadler, A. D. Price, A. N. Zelikin, *Adv. Funct. Mater.*, 2011, **21**, 14.
- 9 A. G. Skirtach, C. Dejumat, D. Braun, A. S. Susa, A. L. Rogach, W. J. Parak, H. M \ddot{o} hwald, G. B. Sukhorukov, *Nano Lett.*, 2005, **5**, 1371.
- 10 K. Ariga, Y. M. Lvov, K. Kawakami, Q. Ji, J. P. Hill, *Adv. Drug Deliver Rev.*, 2011, **63**, 762.
- 11 L. L. del Mercato, M. M. Ferraro, F. Baldassarre, S. Mancarella, V. Greco, R. Rinaldi, S. Leporatti, *Adv. Colloid Interfac.*, 2014, **207**, 139.
- 12 V. Vergaro, F. Scarlino, C. Bellomo, R. Rinaldi, D. Vergara, M. Maffia, F. Baldassarre, G. Giannelli, X. C. Zhang, Y. M. Lvov, S. Leporatti, *Adv. Drug Deliver Rev.*, 2011, **63**, 847.
- 13 W. J. Tong, X. X. Song, C. Y. Gao, *Chem. Soc. Rev.*, 2012, **41**, 6103.
- 14 Y. Jia, Y. Cui, J. Fei, M. Du, L. Dai, J. Li, Y. Yang, *Adv. Funct. Mater.*, 2012, **22**, 1446.
- 15 C. Ganas, A. Weiss, M. Nazareus, S. Rosler, T. Kissel, P. R. Gil, W. J. Parak, *J. Controlled Release*, 2014, **196**, 132.

- 16 R. R. Costa, E. Castro, F. J. Arias, J. C. Rodriguez-Cabello, J. F. Mano, *Biomacromolecules*, 2013, **14**, 2403.
- 17 T. A. Kolesnikova, D. A. Gorin, P. Fernandes, S. Kessel, G. B. Khomutov, A. Fery, D. G. Shchukin, H. Möhwald, *Adv. Funct. Mater.*, 2010, **20**, 1189.
- 18 S. De Koker, B. G. De Geest, C. Cuvelier, L. Ferdinande, W. Deckers, W. E. Hennink, S. De Smedt, N. Mertens, *Adv. Funct. Mater.*, 2007, **17**, 3754.
- 19 C. Y. Jiang, V. V. Tsukruk, *Adv. Mater.*, 2006, **18**, 829.
- 20 L. L. del Mercato, E. Gonzalez, A. Z. Abbasi, W. J. Parak, V. Puntès, *J. Mater. Chem.*, 2011, **21**, 11468.
- 21 C. S. Peyratout, L. Dahne, *Angew. Chem., Int. Ed.*, 2004, **43**, 3762.
- 22 B. G. De Geest, A. G. Skirtach, A. A. Mamedov, A. A. Antipov, N. A. Kotov, S. C. De Smedt, G. B. Sukhorukov, *Small*, 2007, **3**, 804.
- 23 S. Schmidt, P. A. L. Fernandes, B. G. De Geest, M. Delcea, A. G. Skirtach, H. Möhwald, A. Fery, *Adv. Funct. Mater.*, 2011, **21**, 1411.
- 24 M. L. De Temmerman, J. Rejman, B. Lucas, R. E. Vandembroucke, C. Libert, J. Demeester, S. C. De Smedt, *Adv. Funct. Mater.*, 2012, **22**, 4236.
- 25 L. L. del Mercato, P. Rivera-Gil, A. Z. Abbasi, M. Ochs, C. Ganas, I. Zins, C. Sonnichsen, W. J. Parak, *Nanoscale*, 2010, **2**, 458.
- 26 L. Q. Ge, H. Mohwald, J. B. Li, *ChemPhysChem*, 2003, **4**, 1351.
- 27 A. R. Battle, S. M. Valenzuela, A. Mechler, R. J. Nichols, S. Praporski, I. L. di Maio, H. Islam, A. P. Cirard-Egrot, B. A. Cornell, J. Prashar, F. Caruso, L. L. Martin, D. K. Martin, *Adv. Funct. Mater.*, 2009, **19**, 201.
- 28 M. Fischlechner, O. Zschornig, J. Hofmann, E. Donath, *Angew. Chem., Int. Ed.*, 2005, **44**, 2892.
- 29 J. Shao, M. Xuan, L. Dai, T. Si, J. Li, Q. He, *Angew. Chem., Int. Ed.*, 2015, **54**, 12782.
- 30 W. C. Zamboni, V. Torchilin, A. K. Patri, J. Hrkach, S. Stern, R. Lee, A. Nel, N. J. Panaro, P. Grodzinski, *Clin. Cancer Res.*, 2012, **18**, 3229.
- 31 S. Stolnik, L. Illum, S. S. Davis, *Adv. Drug Deliver Rev.*, 2012, **64**, 290.
- 32 A. Parodi, N. Quattrocchi, A. L. van de Ven, C. Chiappini, M. Evangelopoulos, J. O. Martinez, B. S. Brown, S. Z. Khaled, I. K. Yazdi, M. Vittoria Enzo, L. Isenhardt, M. Ferrari, E. Tasciotti, *Nat. Nanotechnol.*, 2013, **8**, 61.
- 33 A. C. Anselmo, C. L. Modery-Pawłowski, S. Menegatti, S. Kumar, D. R. Vogus, L. L. Tian, M. Chen, T. M. Squires, A. Sen Gupta, S. Mitragotri, *ACS Nano*, 2014, **8**, 11243.
- 34 N. E. T. Furman, Y. Lupu-Haber, T. Bronshtein, L. Kaneti, N. Letko, E. Weinstein, L. Baruch, M. Machluf, *Nano Lett.*, 2013, **13**, 3248.
- 35 C.-M. J. Hu, R. H. Fang, K.-C. Wang, B. T. Luk, S. Thamphiwatana, D. Dehaini, P. Nguyen, P. Angsantikul, C. H. Wen, A. V. Kroll, *Nature*, 2015, **526**, 118.
- 36 L.-L. Li, J.-H. Xu, G.-B. Qi, X. Zhao, F. Yu, H. Wang, *ACS nano*, 2014, **8**, 4975.
- 37 C. M. J. Hu, L. Zhang, S. Aryal, C. Cheung, R. H. Fang, L. F. Zhang, *Proc. Natl. Acad. Sci. U. S. A.*, 2011, **108**, 10980.
- 38 M. Baggiolini, *Nature*, 1998, **392**, 565.
- 39 C. E. Lewis, J. W. Pollard, *Cancer Res.*, 2006, **66**, 605.
- 40 M. R. Choi, K. J. Stanton-Maxey, J. K. Stanley, C. S. Levin, R. Bardhan, D. Akin, S. Badve, J. Sturgis, J. P. Robinson, R. Bashir, N. J. Halas, S. E. Clare, *Nano Lett.*, 2007, **7**, 3759.
- 41 T. A. Springer, *Cell*, 1994, **76**, 301.
- 42 S. Mitragotri, J. Lahann, *Nat. Mater.*, 2009, **8**, 15.
- 43 R. Skalak, P. Branemark, *Science*, 1969, **164**, 717.
- 44 J. C. Hogg, C. M. Doerschuk, *Annu. Rev. Physiol.*, 1995, **57**, 97.
- 45 T. J. Merkel, S. W. Jones, K. P. Herlihy, F. R. Kersey, A. R. Shields, M. Napier, J. C. Luft, H. Wu, W. C. Zamboni, A. Z. Wang, *Proc. Natl. Acad. Sci. U. S. A.*, 2011, **108**, 586.
- 46 A. Muñoz Javier, O. Kreft, M. Semmling, S. Kempter, A. G. Skirtach, O. T. Bruns, P. del Pino, M. F. Bedard, J. Rädler, J. Käs, *Adv. Mater.*, 2008, **20**, 4281.